Photoabsorption of Nitrous Oxide through Rydberg States in the Bound and Continuum Spectral Regions: Main Ionization Channels

E. Bustos, A. M. Velasco, I. Martín,* and C. Lavín

Departamento de Química Física, Facultad de Ciencias, Universidad de Valladolid, 47005 Valladolid, Spain

Received: July 12, 2001; In Final Form: October 5, 2001

The oscillator strength spectral density for the partial (through different individual Rydberg series) and total photoabsorption processes which determine the photoionization of N_2O from its ground state has been studied. Despite its relevance for atmospheric chemistry and astrochemistry, only a few data seem to be available in the literature. The molecular-adapted quantum defect orbital (MQDO) method has been employed in the calculations. For the different ionization channels, continuity between the bound and continuum spectral regions has been achieved in the corresponding partial differential oscillator strengths. Good agreement with experiment has been found for the total photoionization cross section.

I. Introduction

Photoabsorption processes are receiving increasing attention both from experimentalists and theoreticians. This may be partly due to their role in atmospheric and interstellar chemistry. Although molecular photoprocesses have long been subjects of experimental study, only relatively recently have synchrotron radiation and equivalent electron-impact sources provided the energetic photons necessary for measurements of partial and fragmented cross sections over wide spectral ranges. These experiments are also supplying a wealth of data to theoreticians as regards the nature and properties of excited electronic states, in particular those that exhibit a Rydberg character. Nevertheless, while the theory of radiation−matter interaction is well established, there is still need for viable computational approximations of photoabsorption intensities.

Nitrous oxide plays an important role in the photochemistry of the Earth's upper atmosphere. It has been found to be involved in the catalytic destruction of ozone in the stratosphere and to be the main source of odd nitrogen, which regulates the ozone layer. The continuous increase in the concentration of N_2O in the Earth's atmosphere constitutes a serious environmental problem in relation to both the thinning of the ozone layer and the greenhouse effect.[1,2] This compound has also attracted attention because of its presence in the interstellar medium.[3] The possibility of N_2O being the only known interstellar compound in which an N atom uses its five valence electrons as such has been the subject of discussion.[4] Upon interaction with photons or electrons, this molecule dissociates asymmetrically into a number of metastable species that can then act as intermediates in atmospheric collision processes. Chemically relevant information can be derived from the spectroscopic behavior of N_2O. For instance, absolute optical oscillator strengths and photoabsorption cross sections for this compound can be used to obtain quantum yields for processes related to its photodissociation.

Some experimental studies of bound−bound transitions in nitrous oxide have been reported.[5,6] A few experimental[7,8] and theoretical[9] data concerning the photoionization of this molecule have also been found in the literature. N_2O has a simple chemical structure, being formed by three second-period atoms, with a total of 16 valence electrons. This fact makes it a good candidate for theoretical investigation. In the present work we have calculated absorption oscillator strengths involving Rydberg states of N_2O and the oscillator strength spectral densities in both the discrete and continuous region of the spectrum for a number of relevant spectral series. The molecular-adapted version of the quantum defect orbital (MQDO) method,[10] which has supplied reliable intensities for Rydberg transitions in a variety of molecular species,[10−16] has been employed. The quantum defect orbital methodology has also proved to yield accurate photoionization cross sections in different atomic systems.[17] The correctness of the present results for nitrous oxide has been assessed with the help of the experimental data available, though scarce, and by the criterion of continuity of the oscillator strength spectral density across the ionization threshold[18] for all the Rydberg series studied.

The complete distribution of the dipole oscillator strength of a molecule is known[18,19] to contain a wealth of information from many points of view, both basic and applied. In addition, the examination of the distribution over the entire spectral range provides an excellent opportunity for finding useful items for further research such as missing gaps in experimental data and the influence of the strength in one spectral domain to optical properties in another. The utility of the complete oscillator strength distribution has been illustrated by us in previous work done with atoms.[17] In this work we have performed the first such comprehensive calculation for a molecular system. In section II we give a brief outline of the computational method. In section III we present the calculated individual absorption oscillator strengths and the oscillator strength distribution, making explicit mention to the contribution of the different photoionization channels from the ground state of N_2O, and compare these data with the available experimental and theoretical results.

It has long been established[20] for Rydberg states in molecules that as excitation increases and the inner loops of the Rydberg molecular orbital become less and less important relative to the outer loops, the Rydberg electron withdraws more and more from influencing the rotational and vibrational motions of the

* Author for correspondence. Tel: +34-983-423272; Fax: +34-983-423013; E-mail: imartin@qf.uva.es

10.1021/jp012678m CCC: $22.00
Published on Web 12/08/2001

nuclei. In the present calculations, we have studied electronic transitions originating and ending in the vibrational ground state of both the upper and lower Rydberg states of nitrous oxide, as these are expected to be the strongest.

II. Method of Calculation

The MQDO technique, formulated to deal with molecular Rydberg transitions has been described in detail elsewhere.[10] A brief summary of this method follows. The MQDO radial wave functions are the analytical solutions of a one-electron Schröedinger equation that contains a model potential of the form

$$V(r)_a = \frac{(c-\delta_a)(2l+c-\delta_a+1)}{2r^2} - \frac{1}{r} \qquad (1)$$

where a represents the set of quantum numbers that define a given molecular state. Solutions of this equation are related to Kummer functions. The parameter δ_a is the quantum defect and c is an integer chosen, within a rather narrow range of values, to ensure the normalization of the orbitals and their correct nodal pattern. The number of radial nodes is equal to $n - l - c - 1$.

The quantum defect, δ_a, is related to the energy eigenvalue of the corresponding state through the following equation:

$$E_a = T - \frac{1}{2(n_a-\delta_a)^2}, \qquad (2)$$

where T is the ionization energy. Both T and E_a are expressed here in Hartrees.

The appropiate radial bound-sate wave functions are the second Whittaker functions

$$R_b(r) = W_{n-\delta,l-\delta+c+1/2}[2Z_{\text{net}}r/n-\delta] \qquad (3)$$

where the index b stands here for bound states. The continuum radial orbitals are also eigenfunctions of the approximate central field potential (1), and can be described by the first Whittaker functions,

$$R_c(r) = M_{Z\text{net}/ik,l-\delta+c+1/2}(2ikr) \qquad (4)$$

where $k = (2E)^{1/2}$ and c denotes the orbitals belonging to the continuum spectral region.

The absorption oscillator strength for a transition between two bound states a and b may be expressed as

$$f(a\rightarrow b) = \frac{2}{3}(E_b - E_a)\, Q\{a\rightarrow b\}|R_{ab}|^2 \qquad (5)$$

The photoionization cross section for a transition between a bound state a and a continuous state b is expressed, in units of megabarns (Mb), as follows:

$$\sigma = 2.6891\left[\frac{Z_{\text{net}}}{(n-\delta)^2} + k^2\right]\frac{1}{2k}Q\{a\rightarrow b\}|R_{ab}|^2 \qquad (6)$$

Equations 5 and 6 should be multiplied by the number of equivalent electrons in the MO that constitutes the initial state, $Q\{a\rightarrow b\}$ are the angular factors resulting from the angular integration and R_{ab} is the radial transition moment. Unlike for atoms, where the angular functions in the QDO model were simply the spherical harmonics, in the MQDO procedure we take symmetry-adapted linear combinations of the former in such a way that the molecular quantum defect orbitals form bases for the different irreducible representations of the molecule's symmetry group. The present calculations for both bound−bound and bound−continuum transitions have all been considered to take place through the electric dipole (E1) mechanism, as this leads to the strongest bands. We have thus adopted the form for R_{ab},

$$R_{ab} = \langle R_a(r)|r|R_b(r)\rangle \qquad (7)$$

For both bound−bound and bound−continuum transitions, the radial transition moments (eq 7) within this model result in closed-form analytical expressions. We find this feature of our method to be one of its major advantages, as it allows the calculation of intensity data free from the convergence problems that plague some self-consistent field procedures. The detailed algebraic expressions for the radial transition moments are given in ref 21, as originally formulated for the photoionization of atomic systems, and in ref 10, as generalized for bound-bound transitions in molecules. Even though the MQDO radial orbitals (eq 3) are meant to describe excited and Rydberg states, they have proved to yield good transition probability estimates when also used for the molecular ground state in the radial transition integral (eq 7).[10−16]

The values of $Q\{a\rightarrow b\}$ for the $C_{\infty v}$ symmetry group, to which the Rydberg states of nitrous oxide belong, are collected in Table 1. In this and the remaining tables we are employing a notation for the molecular Rydberg states that is commonly found in the literature. The $n\,l$ symbol of the atomic orbital to which the molecular Rydberg state can be correlated is followed by its MO character, whenever this is well defined in the molecule, and by the symbol of the irreducible representation to which the Rydberg orbital belongs within the molecular symmetry group (in parentheses). The angular factors collected in Table 1 are rather general for a molecular system belonging to the $C_{\infty v}$ symmetry group and, thus, a specific MO character has been omitted from the Rydberg orbital symbols.

TABLE 1: Values of Non-zero Angular Factors $Q\{a\rightarrow b\}$ for $C_{\infty v}$ Symmetry and for $l = 0, 1, 2$

$Q\{\text{np}\ (\Pi)\rightarrow \text{ns}\ (\Sigma^+)\} = Q\{\text{ns}\ (\Sigma^+)\leftrightarrow \text{np}\ (\Sigma^+)\} = 1/3$
$Q\{\text{ns}\ (\Sigma^+)\rightarrow \text{np}\ (\Pi)\} = 2/3$
$Q\{\text{np}\ (\Sigma^+)\rightarrow \text{nd}\ (\Pi)\} = Q\{\text{np}\ (\Pi)\leftrightarrow \text{nd}\ (\Delta)\} = 2/5$
$Q\{\text{np}\ (\Sigma^+)\leftrightarrow \text{nd}\ (\Sigma^+)\} = 4/15$
$Q\{\text{np}\ (\Pi)\leftrightarrow \text{nd}\ (\Pi)\} = Q\{\text{nd}\ (\Pi)\rightarrow \text{np}\ (\Sigma^+)\} = 1/5$
$Q\{\text{np}\ (\Pi)\rightarrow \text{nd}\ (\Sigma^+)\} = 1/15$
$Q\{\text{nd}\ (\Sigma^+)\rightarrow \text{np}\ (\Pi)\} = 2/15$

III. Results and Analysis

The ground state electronic configuration of N_2O is the following:

$$...(6\sigma)^2\,(1\pi)^4\,(7\sigma)^2\,(2\pi)^4\ \tilde{\chi}\ ^1\Sigma^+$$

The ionization energy (IP) adopted in the present calculations was measured with a pulsed field ionization (PFI) technique by Wiedmann et al.[22] The energy data experimentally determined by Scheper et al.,[23] Patsilinakou et al.,[24] and Lassettre et al.[25] have been employed for the bound Rydberg states. For the continuum orbitals we have used the same quantum defect as that of the highest bound Rydberg state with the same symmetry, given the observed stability of the δ-values along the presently studied spectral series. It may be pointed out that this procedure is strictly limited to the cases that show no signs of level mixing.

In Table 2 we have collected the energy values and quantum defects employed in the present work. In Table 3, the differential

TABLE 2: Energies and Quantum Defects of Bound and Continuum States of N_2O

state	E/cm^{-1}	δ
3s$\sigma(\Sigma^+)$	68557[a]	1.24
4s$\sigma(\Sigma^+)$	91443[b]	1.06
5s$\sigma(\Sigma^+)$	97207[b]	1.01
6s$\sigma(\Sigma^+)$	99692[c]	1.01
7s$\sigma(\Sigma^+)$	101039[c]	1.01
8s$\sigma(\Sigma^+)$	101846[c]	1.02
9s$\sigma(\Sigma^+)$	102378[c]	1.01
∞ s$\sigma(\Sigma^+)$	continuum	1.01
3d$\sigma(\Sigma^+)$	87438[a]	0.43
∞ d$\sigma(\Sigma^+)$	continuum	0.43
3d$\pi(\Pi)$	88027[a]	0.39
∞ d$\pi(\Pi)$	continuum	0.39
3d$\delta(\Delta)$	88972[a]	0.31
∞ d$\delta(\Delta)$	continuum	0.31
	IP = 104097[d]	

[a] Patsilinakou et al.[24] [b] Lasettre et al.[25] [c] Scheper et al.[23] [d] Wiedmann et al.[22]

oscillator strengths, df/dE, for the different photoabsorption channels originating from the ground state are displayed. No comparative data of either experimental or theoretical character have been found in the literature.

In Figures 1−4 we have graphically represented the MQDO oscillator strength spectral density for both the bound and the continuum regions of the spectra corresponding to the 2p$\pi(\tilde{\chi})$ − nsσ (Σ^+), 2p$\pi(\tilde{\chi})$ − ndσ (Σ^+), 2p$\pi(\tilde{\chi})$ − ndπ (Π), and 2p$\pi(\tilde{\chi})$ − ndδ (Δ) Rydberg series. The parts of these data that pertain in the bound spectral region are collected in Table 3. The oscillator strength spectral density, df/dE, in the continuum and the related oscillator strengths, f, in the discrete spectrum have been plotted in the same graph. We have followed a procedure originally developed by Fano and Cooper[18] and later applied

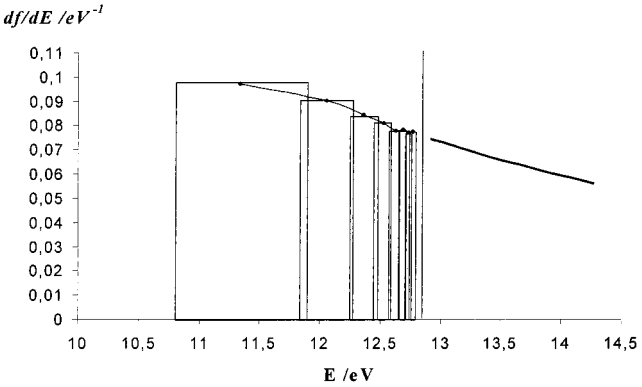

Figure 1. MQDO oscillator strength spectral density for bound and continuum regions of the spectra for the 2p$\pi(\bar{\chi})$ → ns$\sigma(\Sigma^+)$ Rydberg series in N_2O.

by other authors[26,27] and in some of our calculations on atomic systems.[17] The oscillator strengths, or f values, of the discrete transitions are included in the plot in the form of a histogram; that is, a set of rectangular blocks whose respective areas are equal to the f value. The base of each block has a width dE_n/dn^* and is centered at the energy of the corresponding upper state, E_n. The height is then f dn^*/dE_n. The base of each block is $2R/n^{*3}$. The continuous region of the spectrum is included in terms of the spectral density of the oscillator strength, which is related to the photoionization cross section through the expression

$$\sigma(E) = 1.098 \times 10^{-16} \frac{df}{dE} \text{ cm}^2 \text{ eV} \qquad (8)$$

The tops of the blocks in the histogram constructed in this way form a staircase, which constitutes an extrapolation of the

TABLE 3: Differential Absorption Oscillator Strengths for Different Rydberg Ionization Channels of N_2O, in eV^{-1}

E/eV	2p$\pi(\bar{\chi})$→ns$\sigma(\Sigma^+)$	2p$\pi(\bar{\chi})$→nd$\sigma(\Sigma^+)$	2p$\pi(\bar{\chi})$→nd$\pi(\Pi)$	2p$\pi(\bar{\chi})$→nd$\delta(\Delta)$
13.0	0.0731	0.0237	0.0702	0.1360
14.0	0.0594	0.0218	0.0655	0.1297
15.0	0.0489	0.0200	0.0606	0.1221
16.0	0.0408	0.0183	0.0559	0.1141
17.0	0.0343	0.0167	0.0514	0.1060
18.0	0.0292	0.0153	0.0472	0.0985
19.0	0.0250	0.0140	0.0434	0.0914
19.2	0.0242	0.0137	0.0427	0.0901
19.5	0.0232	0.0134	0.0417	0.0881
20.0	0.0215	0.0128	0.0400	0.0849
20.5	0.0200	0.0123	0.0384	0.0818
21.2	0.0182	0.0116	0.0363	0.0777
21.8	0.0168	0.0110	0.0346	0.0743
22.0	0.0163	0.0108	0.0341	0.0733
22.5	0.0153	0.0104	0.0328	0.0707
23.0	0.0143	0.0100	0.0315	0.0682
24.0	0.0127	0.0092	0.0292	0.0636
25.0	0.0112	0.0086	0.0272	0.0593
26.0	0.0100	0.0079	0.0253	0.0555
27.0	0.0089	0.0074	0.0236	0.0519
27.5	0.0085	0.0071	0.0228	0.0503
28.0	0.0080	0.0069	0.0220	0.0487
29.0	0.0072	0.0064	0.0206	0.0457
29.5	0.0069	0.0062	0.0199	0.0443
30.0	0.0065	0.0060	0.0193	0.0430
31.0	0.0059	0.0056	0.0181	0.0405
32.0	0.0054	0.0053	0.0170	0.0381
32.5	0.0051	0.0051	0.0165	0.0370
34.0	0.0045	0.0047	0.0151	0.0340
35.0	0.0041	0.0044	0.0142	0.0322
36.0	0.0038	0.0041	0.0135	0.0305
37.5	0.0033	0.0038	0.0124	0.0282
38.0	0.0032	0.0037	0.0121	0.0275
40.0	0.0027	0.0033	0.0109	0.0249
47.0	0.0017	0.0024	0.0078	0.0180
60.5	0.0008	0.0014	0.0045	0.0107

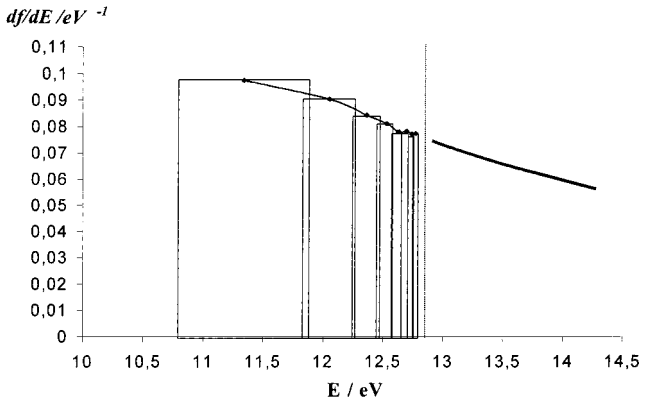

Figure 2. MQDO oscillator strength spectral density for bound and continuum regions of the spectra for the $2p\pi(\tilde{\chi}) \rightarrow nd\sigma(\Sigma^+)$ Rydberg series in N_2O.

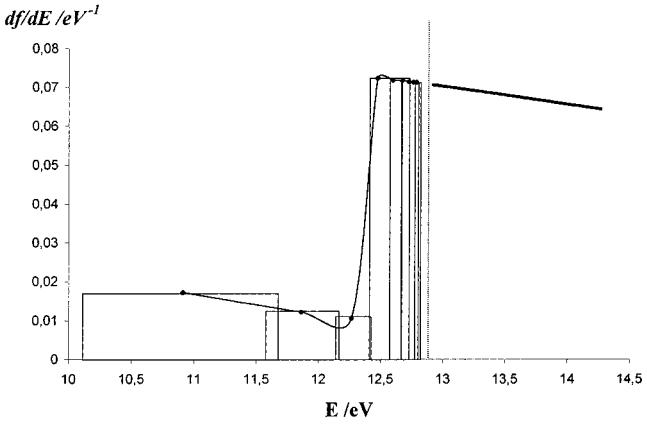

Figure 3. MQDO oscillator strength spectral density for bound and continuum regions of the spectra for the $2p\pi(\tilde{\chi}) \rightarrow nd\pi(\Pi)$ Rydberg series in N_2O.

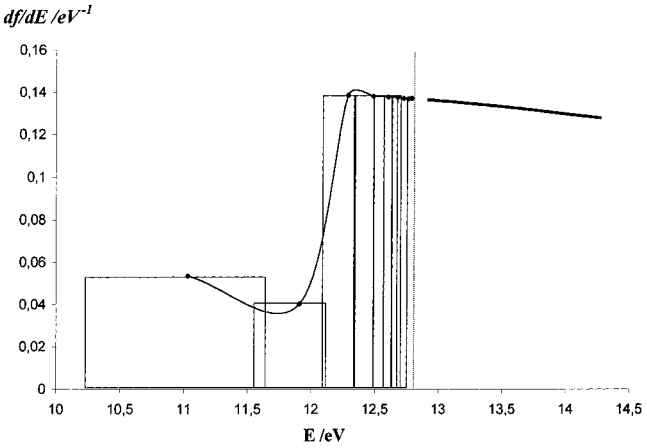

Figure 4. MQDO oscillator strength spectral density for bound and continuum regions of the spectra for the $2p\pi(\tilde{\chi}) \rightarrow nd\delta(\Delta)$ Rydberg series in N_2O.

continuum spectrum below the ionization limit. In other words, the staircase and the continuum oscillator strength should join smoothly across the threshold if the data are correct, as the discrete part of the spectrum for any spectral series can be considered as an appendage of the continuum.[18] It is apparent that the present results depicted in Figures 1 to 4 comply with this requirement, and, thus, the cross section at the photoionization threshold, which could not be directly calculated given that $n = \infty$, may be interpolated from the graphs.

In Figure 5 we have plotted the MQDO partial oscillator strength spectral density for all the Rydberg series of N_2O that constitute the different possible photoionization channels for this molecule in its ground state, covering an energy range of 10 to 60 eV. Our main purpose has been to show the expected monotonic decrease with increasing free electron energy exhibited by all these spectral series in the continuum, given that these series are not expected to suffer from perturbations or autoionization resonances induced by series mixings. This regular behavior may also allow a safe extrapolation of the spectral density at energies higher than reported, if needed, for example, for designing future experiments.

Through inspection of Figures 1−5, we find a complete consistency between the calculated photoionization cross sections and oscillator strengths. In all the Rydberg series, the extrapolation of the *f* values in the discrete spectrum leads to the same point at the ionization threshold as the extrapolation of the oscillator-strength spectral density from the opposite direction (that of decreasing energy). In the absence of comparative data, these features exhibited by the present MQDO data make us feel confident in their, at least qualitative, reliability.

Finally, we depict in Figure 6 the oscillator strength spectral density for the total photoinization from the ground state of N_2O in a range of 12 to 72 eV of photon energy. The total cross section for the photoionization, to which the above property is proportional (eq 8), from a state *i* in a a molecule may be expressed as a sum of partial cross sections that correspond to all compatible absorption processes $i \rightarrow j$,

$$\sigma_i(h\nu) = \sum_j \sigma_{i-j}(h\nu) \tag{9}$$

Making use of this expression, we have determined the total cross section for the ionization from the ground state of N_2O, $2p\pi\tilde{\chi}(^1\Sigma^+)$, through the four compatible ionization channels $2p\pi(\tilde{\chi}) - ns\sigma\ (\Sigma^+)$, $2p\pi(\tilde{\chi}) - nd\sigma\ (\Sigma^+)$, $2p\pi(\tilde{\chi}) - nd\pi\ (\Pi)$, and $2p\pi(\tilde{\chi}) - nd\delta\ (\Delta)$, for which the differential oscillator strengths are collected in Table 3.

In Figure 6, data from the experimental measurements by Brion and Tan,[7] Carlson et al.,[8] and Trueslade and co-workers,[28] as well those obtained in a theoretical calculation with the ground state inversion potential method (GIPM) by Kilcoyne and co-workers,[9] have also been included. Brion and Tan[7] employed the technique known as magic angle (e, 2e), which yields an effective simulation of photoelectron spectroscopy (PES) data. Trueslade et al. employed a synchrotron radiation (SR) in the energy range 19 to 31 eV.[28] These authors pointed out the need for more accurate calculations to ease the assignment of the experimental measurements. Carlson and collaborators,[8] in addition to obtaining cross sections from the angular-resolved spectrum of N_2O, performed theoretical calculations, but these have not been included in Figure 6, given that the experimental data are sufficiently comprehensive for an assessment of the MQDO results. Other theoretical data available in the literature are the calculations by Kilkoyne and co-workers,[9] carried out with two versions of the ground state inversion potential (GIPM) model, with (GIPM/D) and without (GIPM/A) inclusion of multicenter interference effects. The calculations by Carlson et al.[8] and by Kilcoyne et al.[9] are in disagreement with the measurements both in magnitude and trend, except at rather high energies, unlike the present MQDO results, which conform rather well with the observations in the whole energy range.

An inspection of the total MQDO oscillator strength spectral density in the continuum region between 17 and 70 eV, as displayed in Figure 6, reveals a better agreement between the

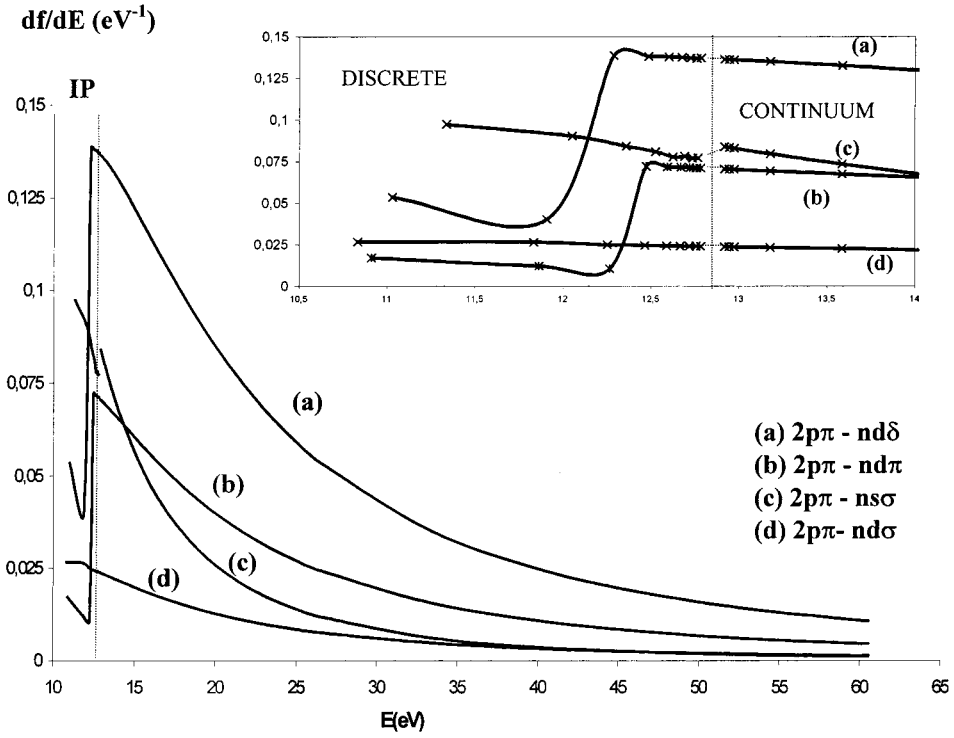

Figure 5. MQDO oscillator strength spectral density corresponding to different Rydberg series of N_2O. (inset) Enlarged spectral region around the ionization threshold.

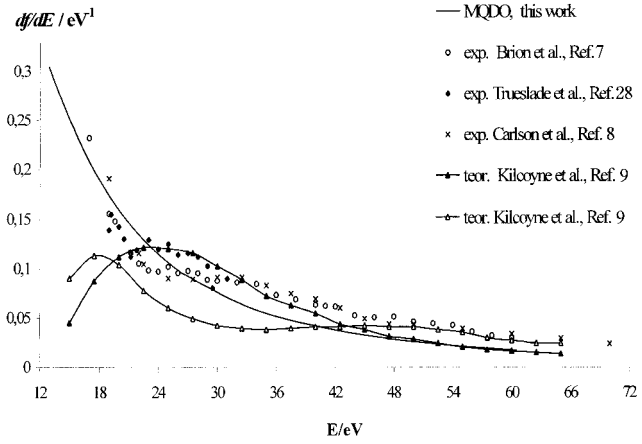

Figure 6. Total oscillator strength spectral density for the photoionization of N_2O from its ground state.

present calculations and the results of the measurements than those observed for other theoretical results.[9] This fact, together with the compliance of the MQDO differential oscillator strengths of continuity through the spectral series limit in all the cases of the present study, leads us to be confident in the adequacy of the MQDO procedure for this type of studies.

IV. Concluding Remarks

In its first application to the photoionization of a molecular system, the molecular adapted quantum defect orbital (MQDO) method has yielded results for nitrous oxide that are, at least, of qualitative correctness for the bound spectral region, where no comparative data seem to be available, and in much better accord with experiment than other theoretical calculations for the continuum. Partial differential oscillator strengths for the different Rydberg series that constitute the ionization channels of N_2O from its ground state have been calculated up to a photon energy of 60.5 eV. These data are supplied, to our knowledge, for the first time.

For the total differential oscillator strength, some experimental and theoretical data have been found in the literature. The closeness, both in magnitude and trend, of the MQDO results to the experimental values, in contrast to that exhibited by the other theoretical results, is shown graphically. This fact, together with the fulfillment of the criterion of continuity by the presently calculated partial differential oscillator strengths across the ionization threshold, makes us feel confident in the quality of our results and, more generally, in the adequacy of the MQDO technique for supplying reliable intensity data in molecular photoionization studies.

Acknowledgment. This work has been supported by the D.G.E.S. of the Spanish Ministry for Science and Technology within Project No. PB97-0399-C03-01. A.M.V. and E.B. also wish to acknowledge their respective research grants from the same institution.

References and Notes

(1) Yung, Y. L.; Miller, C. E. *Science* **1997**, *278*, 1778.
(2) Rahn, T.; Wahlen, M. *Science* **1997**, *278*, 1776.
(3) Turner, B. E. *Symp. Int. Astron. Union* **1992**, *150*, 181.
(4) Wilson, W. J.; Snyder, L. E. *Astrophys. J.* **1981**, *246*, 86.
(5) Huebner, R. H.; Celotta, R. J.; Mielczarek, S. R.; Kuyatt, C. E. *J. Chem. Phys.* **1975**, *63*, 449.
(6) Chan, W. F.; Cooper, C.; Brion, C. E. *Chem. Phys.* **1994**, *180*, 77.
(7) Brion, C. E.; Tan, K. H. *J. Chem. Phys.* **1978**, *34*, 141.
(8) Carlson, T. A.; Keller, P. A.; Taylor, J. W.; Whitley, T.; Grimm, F. A. *J. Chem. Phys.* **1983**, *79*, 97.
(9) Kilcoyne, D. A. L.; Nordlhom, F.; Hush, N. S. *Chem. Phys.* **1986**, *107*, 225.
(10) Martín, I.; Lavín, C.; Velasco, A. M.; Martín, M. O.; Diercksen, G. H. F.; Karwowski, J. *Chem. Phys.* **1996**, *202*, 307.
(11) Martín, I.; Lavín, C.; Karwowski, J. *Chem. Phys. Lett.* **1996**, *255*, 89.
(12) Martín, I.; Lavín, C. Martín, I.; Lavín, C. *Adv. Quantum Chem.* **1997**, *28*, 205.
(13) Velasco, A. M.; Martín, I.; Lavín, C. *Chem. Phys. Lett.* **1997**, *264*, 579.
(14) Martín, I.; Lavín, C.; Pérez-Delgado, Y.; Karwowski, J.; Diercksen, G. H. F. *Adv. Quantum Chem.* **1998**, *32*, 181.

(15) Martín, I.; Lavín, C.; Velasco, A. M. *Adv. Quantum Chem.* **2001**, *39*, Part I, 146.
(16) Martín, I.; Lavín, C.; Pérez-Delgado, Y. *Chem. Phys. Lett.* **1999**, *305*, 178.
(17) Barrientos, C.; Martín, I. *Can. J. Phys.* **1988**, *66*, 29, and references therein.
(18) Fano, U.; Cooper, J. W. *Rev. Mod. Phys.* **1968**, *40*, 441.
(19) Kosman, W. M.; Wallace, S. *J. Chem. Phys.* **1985**, *82*, 1385.
(20) Mulliken, R. S. *J. Am. Chem. Soc.* **1964**, *86*, 3183.
(21) Martín, I.; Simons, G. *J. Chem. Phys.* **1975**, *62*, 4799.
(22) Wiedmann, R. T.; Grant, E. R.; Tonkyn, R. G.; White, M. G. *J. Chem. Phys.* **1991**, *95*, 746.
(23) Scheper, C. R.; Kuijt, J.; Burna, W. J.; de Lange, C. A. *J. Chem. Phys.* **1998**, *109*, 7844.
(24) Patsilinakou, E.; Wiedmann, R. T.; Fotakis, C.; Grant, E. R. *J. Chem. Phys.* **1989**, *91*, 3916.
(25) Lassettre, E. N.; Skerbele, A.; Dillon, M. A.; Ross, K. J. *J. Chem. Phys.* **1968**, *48*, 5066.
(26) Parkinson, W. H.; Reeves, E. M.; Tomkins, F. S. *J. Phys. A* **1976**, *9*, 157.
(27) Lin, C. D. *Astrophys. J.* **1974**, *187*, 385.
(28) Trueslade, C. M.; Southworth, S.; Kobrin, P. H.; Lindle, D. W.; Shirley, D. A. *J. Chem. Phys.* **1983**, *78*, 7117.